water

MDPI

Article

Tidal Level Prediction Model Based on VMD-LSTM Neural Network

Saihua Huang [1], Hui Nie [1,*], Jiange Jiao [2], Hao Chen [1] and Ziheng Xie [2]

[1] College of Hydraulic and Environmental Engineering, Zhejiang University of Water Resources and Electric Power, Hangzhou 310018, China; huangsh@zjweu.edu.cn (S.H.); chenhao@zjweu.edu.cn (H.C.)
[2] College of Mechanical and Electrical Engineering, China Jiliang University, Hangzhou 310018, China; careerjiao@cjlu.edu.cn (J.J.); p23010854133@cjlu.edu.cn (Z.X.)
* Correspondence: nieh@zjweu.edu.cn

Abstract: The fluctuation of the tide is closely related to the production and life of people in coastal areas, and the change in the tide level will have a significant impact on the safety of infrastructure, ship travel, ecological environment, and other issues. Therefore, it is of great significance to analyze, study, and forecast the change in tide level. Aiming at the complex characteristics of nonlinearity, time-varying dynamics, and uncertainty generated by celestial bodies' movements and influenced by geographical as well as hydrometeorological factors, this paper proposes a combined model based on variational mode decomposition (VMD) and long short-term memory neural networks (LSTM). A tidal level prediction procedure is proposed by combining the harmonic analysis method with a neural network and takes the point tide data of Luchao Port from 2021 to 2022 as the applied data. First, the VMD algorithm decomposes the tidal level data into model components. Then, the LSTM model is used to predict each component. Finally, the predicted value of each component is superposed to obtain the final prediction result. Standard evaluation indexes were used to analyze the performance of the proposed model. The model's RMSE, MAE, MAPE, and R^2 were 0.0385, 0.0267, 5.8327, and 99.91%, respectively, superior to other compared models (BP, SVM, and LSTM). This study can provide a reference for tidal level prediction. These results show that the VMD-LSTM model is an effective and reliable tidal level prediction tool with considerable potential in offshore engineering and maritime management.

Keywords: tidal prediction; variational mode decomposition; intrinsic mode functions; long short-term memory neural networks

Citation: Huang, S.; Nie, H.; Jiao, J.; Chen, H.; Xie, Z. Tidal Level Prediction Model Based on VMD-LSTM Neural Network. *Water* **2024**, *16*, 2452. https://doi.org/10.3390/w16172452

Academic Editor: Paul Kucera

Received: 1 July 2024
Revised: 10 August 2024
Accepted: 27 August 2024
Published: 29 August 2024

1. Introduction

Tides, influenced by the gravitational forces of the moon and sun, significantly affect coastal areas' economy and ecology [1]. The study of tidal change is very important for the exploitation of marine resources, disaster warning, and the construction of engineering projects [2]. Accurate tide forecasting is important to ensure safe navigation and efficient use of port resources, and prediction errors can lead to serious maritime accidents [3,4].

In tidal prediction, standard methods include hydrodynamic models, harmonic analysis, and mathematical models. With the development of artificial intelligence, deep learning is gradually being applied to tidal prediction. Predicting tides using hydrodynamic models holds a prominent position. For instance, Luo et al. [5] utilized the MIKE21 hydrodynamic model to predict tides on the coast of Zhejiang. Yin et al. [6] combined the ADCIRC hydrodynamic model with the SWAN model to predict the maximum significant wave heights in Houshui Bay effectively. Yang et al. [7] proposed a multi-stage forecasting system for daily ocean tidal energy. Zhang et al. [8] combined non-stationary harmonic analysis with a deep-learning neural network model to improve tidal forecasts in tidal rivers and estuaries. Additionally, mathematical–statistical methods, such as the traditional tidal harmonic analysis [9], based on the least squares method, calculate the harmonic constants

for each tidal component—amplitude and phase—and subsequently use them to predict tidal levels [10]. Thomas et al. [11] presented a hybrid model for the short-term online tidal current forecast, in which harmonic residual analysis (HRA) and singular spectrum analysis (SSA) are integrated. Wang [12] improved the tidal harmonic analysis method by employing a stepwise regression approach and quadratic analysis techniques. Simultaneously, through the individual analysis and discrimination of multiple tidal components, the optimal tidal component combination was selected to enhance the reliability of the computational results. However, the tidal harmonic analysis method can only predict tidal variations caused by gravitational forces from celestial bodies, such as the sun and the moon. In practical situations, non-astronomical factors such as atmospheric pressure, wind speed, wind direction, water temperature, continental shelves, and coastal topography can significantly impact tidal changes [13,14]. Therefore, harmonic analysis methods may not effectively adapt to fundamental environmental factors.

As a result, methods that separate astronomical tidal factors from non-astronomical tidal factors have gained widespread application. Zhang et al. [15] employed the Grey–GMDH and harmonic analysis models to simulate and separately predict the non-astronomical and astronomical components of tides. The predicted results of these two components were then integrated to form the final tidal forecast. With the advancement of mathematical applications, many more precise mathematical models have continuously emerged and been employed in tidal prediction work. Examples include Gaussian processes, autoregressive integrated moving average models (ARIMA), and others. Abdollah Kavousi-Fard [16] utilized the ARIMA model for tidal prediction in Canada's Fundy Bay. To capture the maximum linear components, appropriate orders for the ARIMA model were determined using the Akaike Information Criterion, effectively enhancing the accuracy of tidal level predictions.

In recent years, with the rapid development of deep learning, algorithms such as Back-propagation (BP) [17], CEEMDAN [18,19], Support Vector Machine (SVM), and Nonlinear Autoregressive with eXogenous inputs (NARX) have gradually found applications in tidal prediction. He et al. [20] employed the BP neural network to predict tidal data in the Cangqian station of the Qiantang River, achieving effective short-term tidal forecasts. Yao et al. [21] established a Support Vector Machine (SVM) tidal prediction model to forecast the average daily tidal level of Sanjiangying station. Nunno [22] and colleagues applied the NARX network to conduct tidal prediction experiments at three different observation points in the Venice Lagoon. Long short-term memory (LSTM) is a variant of recurrent neural networks (RNNs) that can selectively remember or forget information [23]. It addresses issues such as gradient vanishing, gradient exploding, and insufficient long-term memory capacity in RNNs [24], leading to fast convergence when handling long-time-series problems. This enables neural networks to utilize temporal information over extended periods effectively. The LSTM model, by adapting to the data's temporal features and dynamic changes in hydrological processes, can capture long-term dependencies and nonlinear correlations in time series, demonstrating excellent performance in tidal prediction [25]. Yang et al. [26] established a tidal prediction model based on the LSTM neural network. Tidal prediction experiments in locations such as Rizhao, Sanya, and Beihai indicated that the model can achieve reliable forecasting results. Liu et al. [27] utilized a multivariate LSTM neural network to establish a storm surge prediction model at the Chiwan tidal station in Shenzhen, effectively predicting abnormal tidal changes caused by tropical storms. Xu et al. [28] combined the LSTM neural network with the non-stationary harmonic analysis method, achieving accurate predictions for the tidal level at the Nanjing station. Stefanos et al. [29] applied the LSTM method to improve the accuracy of storm surge prediction. Ian et al. [30] introduced the bidirectional attention-based long short-term memory (LSTM) storm surge architecture, BALSSA, improving the accuracy of storm surge predictions.

In practical tidal prediction scenarios, monitoring sensors operate in complex and variable environments, and data with specific errors is a common occurrence. To address this, many scholars have combined neural networks with signal decomposition techniques to reduce the impact of information noise on prediction results, thereby enhancing prediction accuracy.

Standard decomposition algorithms include wavelet decomposition (WPD), empirical mode decomposition (EMD). Liu et al. [31] proposed a tidal prediction model based on wavelet decomposition and ARIMA, using wavelet decomposition to eliminate noise in tidal time series and better restore the nature of tidal movement. EMD is a method for analyzing nonlinear and non-stationary data [32]. Its most significant feature is overcoming the lack of adaptability of base functions [33]. Unlike the Fourier and wavelet transform [34], the EMD process is a finite filtering process that does not require the pre-specification of any base functions [35]. Yin et al. [36], when applying neural network models for tidal prediction, first used the EMD method to preprocess tidal time-series data for stabilization, resulting in more accurate prediction results. Tao et al. [37] pointed out that the Local-EMD-WaveNet model can accurately capture the peaks and troughs of waveforms when the wave height changes considerably. However, mode aliasing and spurious components often occur in EMD-like decomposition algorithms. Therefore, using variational mode decomposition (VMD) to process ammonia nitrogen sequences can decompose complex ammonia nitrogen sequences into modal components of a particular frequency and effectively suppress the mode aliasing phenomenon [38]. Zhang et al. [39] proposed a hybrid variational mode decomposition (VMD) and one-dimensional convolutional neural network (1D-CNN) model (VMD-CNN) for non-stationary wave forecasting. Wang [40] proposes a hybrid model combining improved empirical wavelet transform decomposition (IEWT) and long short-term memory networks (LSTM) for predicting significant wave heights. Ban et al. [41] propose a model that combines the variational mode decomposition (VMD) algorithm with the long short-term memory (LSTM) neural network to predict tidal levels.

In the past, the neural network method applied to predicting tidal level is relatively simple, but the combination and improvement of the machine learning algorithm is expected to improve the prediction accuracy. In light of this, the core of this study is to explore the application effect of the combination of modal decomposition algorithm and neural network model in tidal prediction. Compared with the basic neural network algorithm, the combined model used in this paper can utilize the advantages of VMD algorithm in signal noise reduction and feature extraction, and can effectively reduce signal interference in data, thus improving the prediction accuracy. In this paper, a tidal prediction model based on the combination of VMD and LSTM neural networks is constructed, and the superiority of this model is verified by comparing it with other neural network models and combined models. Compared with Ban et al. [41], the comparison of VMD-LSTM with other basic models and combined models was added in this paper to fully verify the superiority of the combined model in tidal prediction.

2. Materials and Methods

2.1. Data Normalization

Normalization is a method to simplify calculations by representing all attributes in the same measurement unit. It involves using a standard scale or range, assigning equal weights to all data attributes, facilitating easier comparisons and aggregations, and improving data convergence conditions [42,43]. In tidal sequence prediction, it is necessary to perform normalization on input data in advance to eliminate the influence of dimensional and value range differences between indicators. This involves scaling the data proportionally to fall within a specific range, enabling comprehensive analysis [44].

This study will employ the Min-Max normalization algorithm to preprocess tidal data. Min-Max normalization, or linear function normalization, entails a linear transformation of the original data. Equation (1) maps the original data to the range [0, 1], preserving the original data distribution without alteration.

$$x_{new} = \frac{x - x_{min}}{x_{max} - x_{min}}, \quad (1)$$

where the data to be normalized is represented by x, and x_{new} denotes the data after Min-Max normalization. x_{max}, x_{nin} represent the maximum and minimum values within the current dataset.

2.2. Variational Mode Decomposition

VMD is an adaptive non-recursive signal decomposition method that synthesizes the problems existing in EMD and EEMD and improves on this basis to improve the mode aliasing and end effect problems. The VMD algorithm can decompose the original data $f(t)$ into K modal components whose center frequency is ω_k with limited bandwidth and can effectively extract the information of the original data at different frequencies. The steps of the VMD algorithm are as follows:

(1) Construct a variational problem. For each mode, the associated analytical signal ($u_k(t)$) is computed by a Hilbert transform to obtain a unidirectional spectrum. Then, each analytic signal is combined with the center frequency ($e^{-j\omega_k t}$) and modulated to the corresponding baseband. Finally, the above signal gradient squared L2 norm is calculated to obtain a constrained model, as shown in Equation (2).

$$\begin{cases} \min\limits_{\{u_k\}\{\omega_k\}} \left\{ \sum_{k=1}^{K} \| \partial_t \left[\left(\delta(t) + \frac{j}{\pi t} \right) * u_k(t) \right] e^{-j\omega_k t} \|_2^2 \right\} \\ s.t. \sum_{k=1}^{K} u_k(t) = f(t) \end{cases} \tag{2}$$

where u_k represents the decomposition modal component; * represents the convolution operator; ω_k represents the center frequency of each modal component; ∂_t is the partial derivative of time.

(2) Solve the variational problem. By introducing the Lagrange multiplication operator λ and penalty factor α, the constrained model is transformed into an unconstrained variational model:

$$\begin{aligned} &L\left(\{u_k\}, \{\omega_k\}, \lambda\right) = \\ &\alpha \sum_{k=1}^{K} \| \partial t \left[\left(\delta(t) + \frac{j}{\pi t} \right) * u_k(t) \right] e^{-j\omega_k t} \|_2^2 \\ &+ \| f(t) - \sum_{k=1}^{K} u_k \|_2^2 + \left\langle \lambda(t), f(t) - \sum_{k=1}^{K} u_k \right\rangle \end{aligned} \tag{3}$$

In order to obtain the optimal value of the constrained variational model, the alternating direction multiplier iterative algorithm is used to update the u_k and ω_k expressions, and the termination conditions are as follows:

$$\sum_{k=1}^{K} \frac{\| u_k^{n+1} - u_k^n \|}{\| u_k^n \|^2} < \varepsilon, n < N \tag{4}$$

$$u_k^{n+1}(k) = \frac{f(\omega) - \sum_{i \neq k}^{K} u_i^n(\omega) + \frac{\lambda^n(\omega)}{2}}{1 + 2\alpha\left(\omega - \omega_k^n\right)^2} \tag{5}$$

$$\omega_k^{n+1} = \frac{\int_0^\infty \omega \left| u_k^n(\omega) \right|^2 d\omega}{\int_0^\infty \left| u_k^n(\omega) \right|^2 d\omega} \tag{6}$$

where n is the number of iterations; $f(\omega)$, $u_i^n(\omega)$ and $\lambda^n(\omega)$ represent the Fourier change in $f(t)$, $u_i^n(t)$ and $\lambda^n(t)$, respectively; N indicates the maximum number of iterations.

In this paper, we use the PyVMD toolkit in Python to conduct experiments. PyVMD is a Python library specially developed for MD decomposition and provides a complete set of VMD implementation methods, including signal preprocessing, VMD, and result analysis.

2.3. Long Short-Term Memory Neural Network

2.3.1. Basic Principles of RNN

In a traditional feedforward neural network, data streams are delivered hierarchically through input, hidden, and output layers. Because of its structural characteristics, the

traditional feedforward neural network has been widely used in computer intelligent recognition. Similarly, due to the independent structure between the layers, there is no connection between them, and it is impossible to analyze the current information through historical information. Therefore, few scholars have studied the time series data through the traditional feedforward neural network. To solve this problem, recurrent neural networks (RNNs) have emerged, the structure of which is shown in Figure 1. It can be seen that there are connections between the cells of the network, demonstrating its ability to analyze and process time-series data problems.

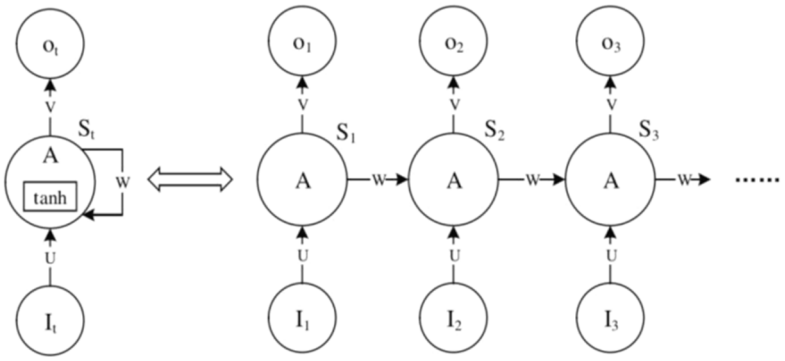

Figure 1. RNN structure diagram. Where t represents the time scale, I is the input information, and S is the memory formed with storage function, which is calculated by the current input information and historical processing information; O is the output information obtained through the current memory calculation analysis; U, V, and W are the three network weights. The tanh is a common activation function in the field of deep learning that maps the input real numbers to the range −1 to 1. As can be seen from the figure, each cell of the recurrent neural network has a state line pointing to itself. This state line increases the information stacking capability of the neural network based on the feedforward neural network, and there are new inputs and outputs in each time state. This unique structure enables it to deal with the problem of the connection between the input content before and after.

Although the traditional recurrent neural network can effectively solve the problem of feedforward neural networks, there are some defects in the network parameter training process of the traditional recurrent neural network. For the problem consisting of a long period, its derivation rule will gradually reduce the derivation result until it is ignored, when the network weight will stop updating, and the model training will fail. The calculation results of some distant nodes are ignored due to the influence of distance, which is the so-called phenomenon of gradient disappearance. Therefore, the ordinary recurrent neural network cannot analyze and store data with a long history, nor can it deal with the current problem effectively.

2.3.2. Basic Principles of LSTM

The structure of the LSTM neural network improves the original traditional recurrent neural network. It can analyze the correlation between the two kinds of data and has multiple spatial and time dimensions.

In the LSTM architecture, three unique structures endow it with the ability to handle correlations in long-time sequences. These structures are known as the "forget gate", "input gate", and "output gate". An extra memory cell C_t is also introduced alongside the regular output h_t at each unit. This memory cell selectively carries memory backward through each layer, significantly enhancing the memory capacity of the LSTM [45]. The structure of the LSTM network is illustrated in Figure 2.

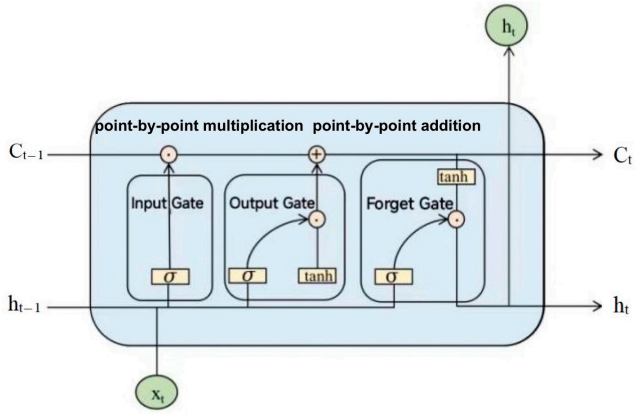

Figure 2. LSTM structure diagram.

(1) Forget Gate: The role of the forget gate is to determine which information to discard from the cell state at the current time step. It generates an output between 0 and 1 through a sigmoid function, where 0 indicates complete forgetting, and 1 indicates complete retention. This gate aims to enable the model to autonomously learn and decide when to forget past information, facilitating the handling of extended sequential information.

$$F_t = \sigma\Big(W_f[h_{t-1}, x_t] + b_f\Big) F_t = \sigma\Big(W_f[h_{t-1}, x_t] + b_f\Big), \tag{7}$$

where F_t represents the value of the forget gate, which determines the information to be discarded from the cell state at the current time step. The computation of the forget gate involves several components: x_t denotes the information input at the current time step, h_{t-1} represents the output of the unit from the previous time step, W_f is the weight matrix of the forget gate, b_f is the bias term associated with the forget gate, and σ denotes the "sigmoid" activation function.

(2) Input Gate: The input gate updates the content within the cell state. It amalgamates the input at the current time step with the hidden state from the previous time step, generating an output from 0 to 1 through the sigmoid function. Simultaneously, it produces a candidate value that encapsulates the current input information using the *tanh* function. The amalgamation of these two components constitutes a candidate update for the cell state at the current time step. Subsequently, the output of the input gate determines the extent to which the candidate update should be assimilated into the cell state.

$$I_t = \sigma(W_t \cdot [h_t - 1, x_t] + b_t), \tag{8}$$

$$\widetilde{C}_t = tanh(W_c \cdot [h_t - 1, x_t] + b_c), \tag{9}$$

$$C_t = f_t \cdot C_t - 1 + I_t \cdot \widetilde{C}_t. \tag{10}$$

where I_t represents the value of the input gate, W_t is the weight matrix of the input gate, b_t is the bias term of the input gate, denotes the updated information at the current time step, W_c is the weight matrix of the cell state, b_c is the bias term of the cell state, and *tanh* denotes the hyperbolic tangent activation function, which produces a new cell state value.

(3) Output Gate: The output gate determines the hidden state at the current time step. It generates an output between 0 and 1 through the sigmoid function, deciding which part of the cell state will be output at the current time step. A portion of the cell state is used to calculate the hidden state at the current time step. This hidden state is then transmitted to the next time step and, when necessary, output to the external network.

$$O_t = \sigma(W_o \cdot [h_t - 1, x_t] + b_o), \tag{11}$$

$$h_t = O_t \cdot tan(C_t). \tag{12}$$

where O_t represents the value of the output gate, h_t is the current time step's unit output information, W_o is the weight matrix of the output gate, and b_o is the bias term of the output gate.

2.4. VMD-LSTM Model

The flowchart of the tidal level prediction model, which combines variational mode decomposition (VMD) with long short-term memory (LSTM) neural networks, is illustrated in Figure 3. The network structure diagram of the model is shown in Figure 4. The construction of the model primarily involves three main components:

(1) Preprocess the data using the Min-Max normalization algorithm.
(2) Decompose the original tidal level data using variational mode decomposition (VMD) to obtain k intrinsic mode functions.
(3) Utilize the long short-term memory (LSTM) neural network model to independently predict each *IMF* component (IMF_i) and the residual (RES). Finally, the predicted results of each *IMFi* component are summed up with the residual RES to obtain the ultimate tidal level prediction.

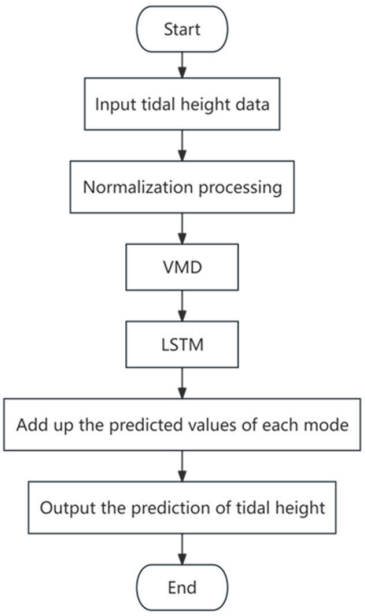

Figure 3. Flowchart of the combined model.

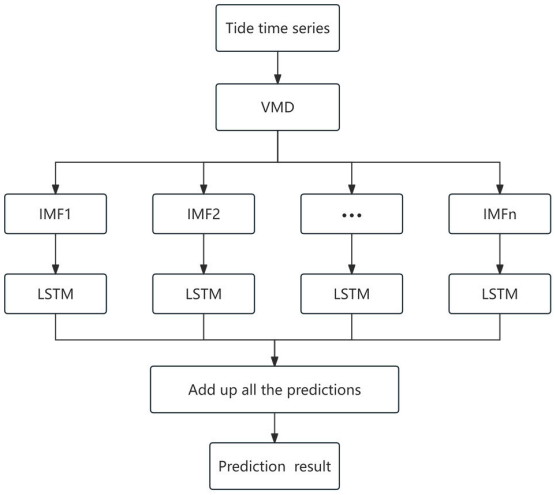

Figure 4. VMD-LSTM combined model structure diagram.

3. Example Analysis

3.1. Data Source

The data utilized in this study are derived from the measured tidal level data at the Lu Chaosha Tide Gauge Station, located in Lingang, Shanghai, in the northern part of Hangzhou Bay. Hangzhou Bay is a typical horn-shaped bay, wide outside, narrow inside, deep outside, and shallow inside. The estuary of the river is 100 km wide; to the west, toward Ganpu, the width is reduced to more than 20 km, the shrinkage rate is 1:1, the water depth in the bay is mostly about 10 m, the tide waves spread into the bay, and the reflection of the two sides makes the tidal range increase. Hangzhou Bay fluctuates twice a day with a period of 745 min. The day tide is different from the night tide. The night tide is larger than the day tide from spring to the autumn equinox. The daily tide is more significant from the autumn equinox to the next spring equinox. The experimental dataset consists of hourly tidal level data from 1 January 2021 to 31 December 2022, totaling 17,520 records. The distribution of the data is illustrated in Figure 5. In order to show the details and features in the original data more clearly, the tidal level data of the first 1000 h in the original data were selected and mapped separately, as shown in Figure 6.

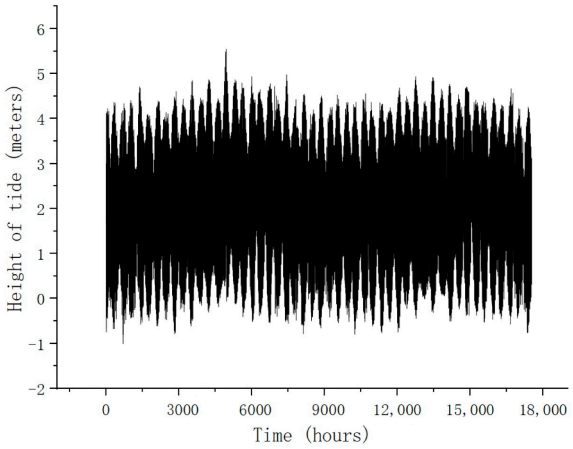

Figure 5. Distribution of tidal level data.

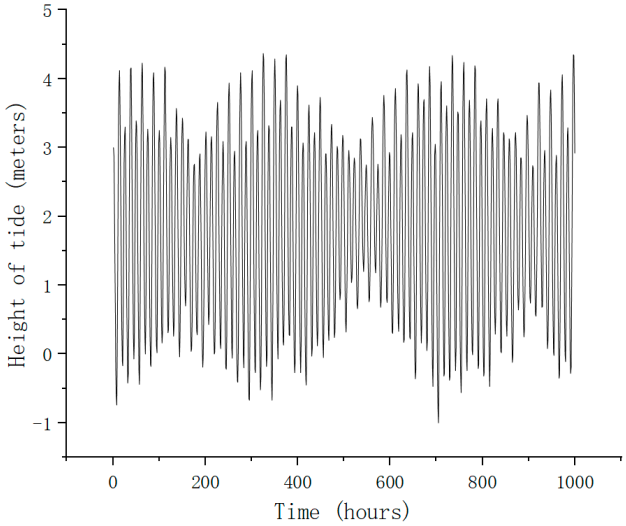

Figure 6. Distribution of tidal level data in the local time.

3.2. VMD

After research and experimental tests, combined with the previous research methods of BAN [30] and Zhao [46], we set the modal decomposition number K of VMD to 4 and the penalty factor α to 2000.

As evident from Figure 4, the tidal level data sequence exhibits nonlinearity and non-stationarity. The variational mode decomposition (VMD) method is employed to mitigate the complexity of the original data sequence. The results of the VMD are depicted in Figure 7.

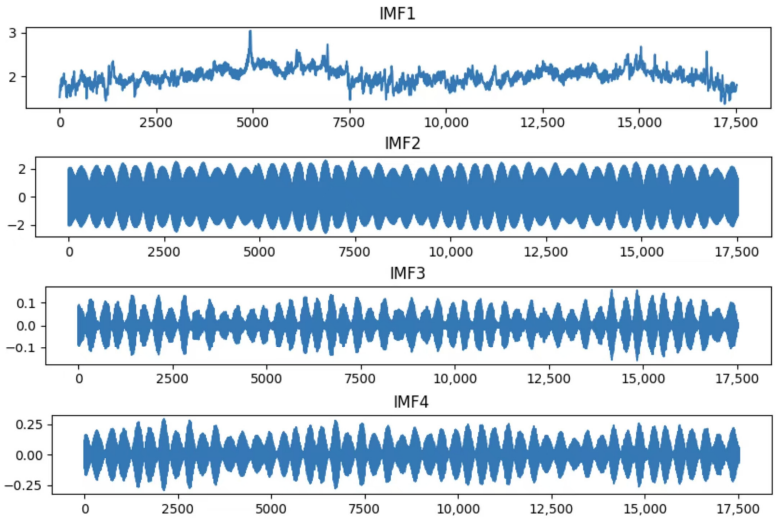

Figure 7. VMD results of tidal level data.

As shown in Figure 7, IMF_1 to IMF_4 are modal components decomposed from the original sequence using VMD. These four modal components reflect the local features of the data at different time scales. After VMD, the non-stationarity of the tidal level time series data is significantly reduced, effectively mitigating the prediction errors caused by tidal level fluctuations. Using the LSTM prediction model to independently forecast each local feature achieves non-interfering effects, enhancing prediction accuracy.

3.3. Prediction Results and Analysis

Four modal components are obtained through VMD, input into the LSTM network for prediction. During the experiment, the first 70% of the data are divided into the training set, and the last 30% are divided into the test set. We adopted the Sparrow search optimization algorithm to determine the value of LSTM hyperparameters [47]. After optimization, the number of hidden layer neurons was 100, the epochs value was 99, the batch_size value was 42, and the learning rate was 0.007. Based on empirical knowledge and multiple experimental results, this study configured the LSTM model hyperparameters as follows: 32 neurons in the hidden layer, 50 epochs, a batch size of 16, a learning rate of 0.001, and a time-window size of 12.

The neural network model in this paper utilized a sliding time window to construct samples. The width of the sliding window was set to 12, implying the use of the tidal data from the previous 11 time points to predict the tidal height at the next time point. Through the continuous movement of the sliding window, shifting one data unit length at a time, a series of overlapping sample data was formed. This approach is highly suitable for handling time-series data, effectively utilizing temporal information while mitigating temporal variability.

As shown in Table 1, after several experimental tests, it can be seen that when the sliding window is set to 12, the error of the model prediction value is the smallest, so the size of the sliding window is determined to be 12 during data segmentation.

Table 1. Comparison of different sliding window sizes.

Sliding Window	RMSE	MAE	MAPE	R^2
2	0.1602	0.1424	12.545	0.9511
3	0.1554	0.1324	12.002	0.9547
4	0.1385	0.1217	11.754	0.9583
5	0.1404	0.1235	11.781	0.9571
6	0.1322	0.1054	10.855	0.9642
7	0.1275	0.1022	10.843	0.9663
8	0.1281	0.1014	10.837	0.9666
9	0.1180	0.0945	10.115	0.9734
10	0.1103	0.0912	9.854	0.9773
11	0.1012	0.0905	9.801	0.9814
12	0.0965	0.0844	9.527	0.9889
13	0.0982	0.0895	9.912	0.9809
14	0.1194	0.1025	10.154	0.9701
15	0.1162	0.1011	10.038	0.9720
16	0.1245	0.1067	10.845	0.9653

The VMD-LSTM model proposed in this study is compared with six commonly used models: BP, SVM, LSTM, EMD-LSMT, EEMD-LSTM, and CEEMDAN-LSTM. The prediction results of each model are depicted in Figure 8. Only 100 sampling points have been selected for demonstration in this section to enhance the visibility and clarity of the prediction result charts.

Figure 8 shows that the predictive values of the VMD-LSTM model used in this study are closer to the actual values than other models. Furthermore, upon closer examination of specific sampling points (top left corner), it is evident that the VMD-LSTM model outperforms traditional BP, SVM, and LSTM neural network models in predicting data peaks and troughs. As can be seen from the local detail zoom in the upper left corner of Figure 9, compared with other basic models, VMD-LSTM can better capture the high complexity and irregularity of tidal time-series data, and the predicted results are more consistent with the actual values with less error. It is suggested that the VMD method can effectively improve the data quality, make it better fit the training data, and predict the unknown data more accurately, which is conducive to the subsequent tide prediction.

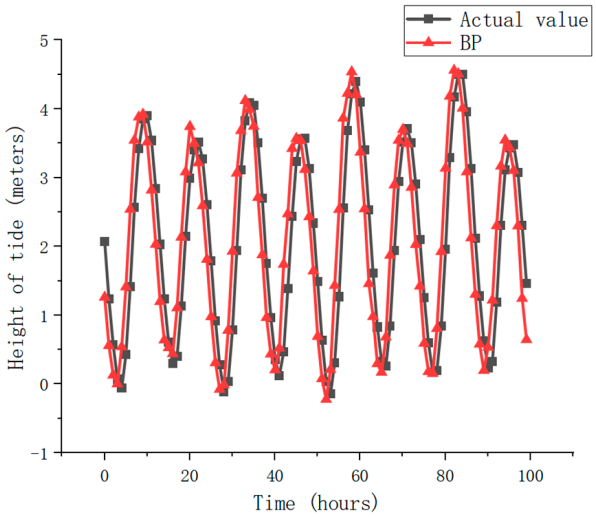

(**a**) Comparison between BP forecast results and actual values.

Figure 8. *Cont.*

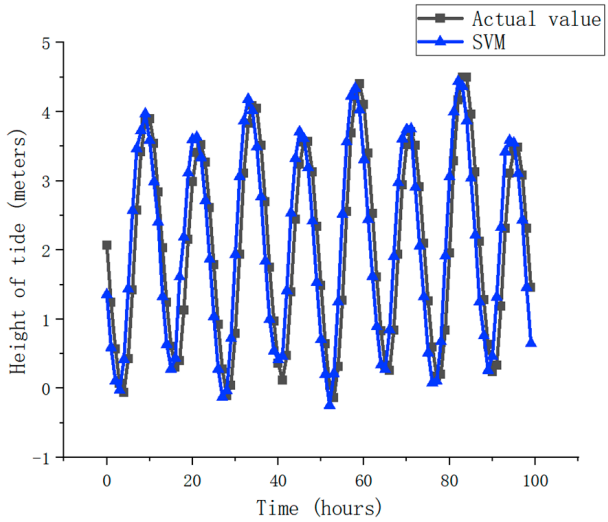

(**b**) Comparison between SVM forecast results and actual values.

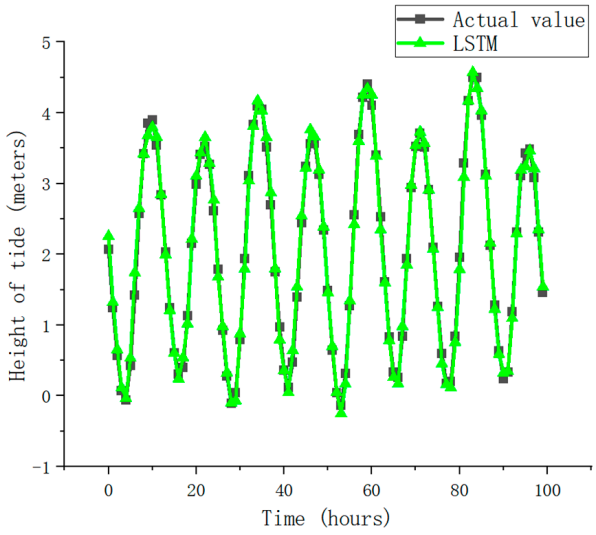

(**c**) Comparison between LSTM forecast results and actual values.

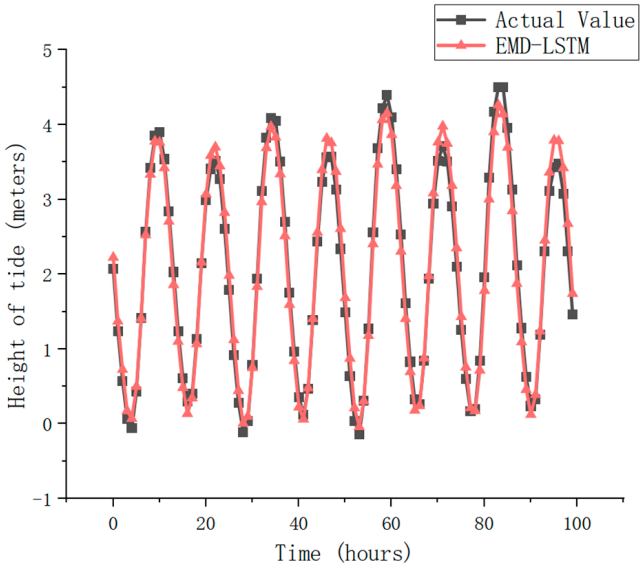

(**d**) Comparison between EMD-LSTM forecast results and actual values.

Figure 8. *Cont.*

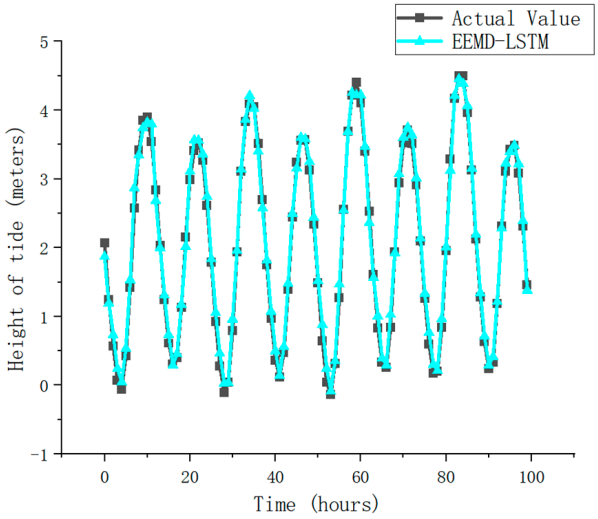

(**e**) Comparison between EEMD-LSTM forecast results and actual values.

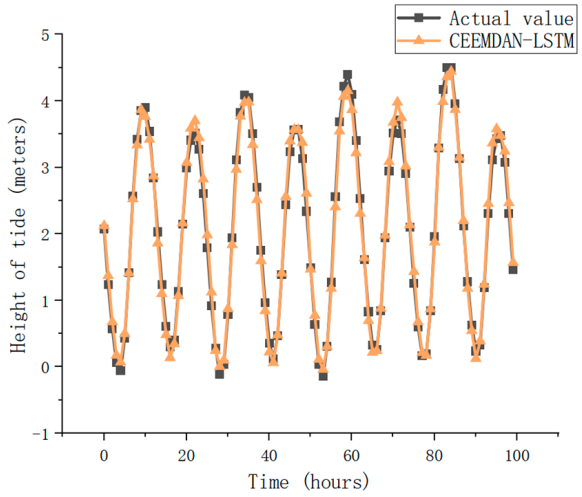

(**f**) Comparison between CEEMDAN-LSTM forecast results and actual values.

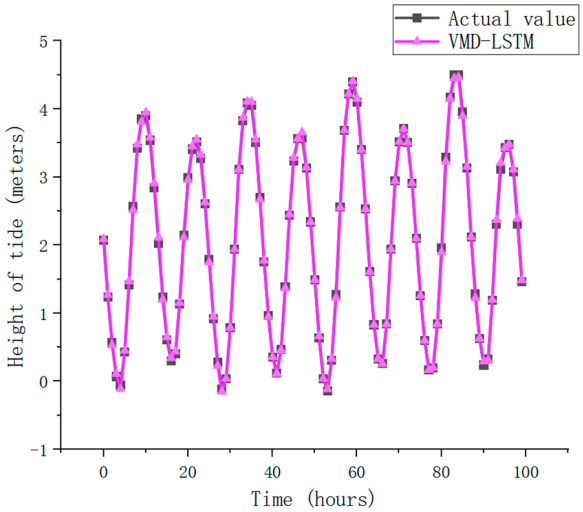

(**g**) Comparison between VMD-LSTM forecast results and actual values.

Figure 8. Prediction results of different models.

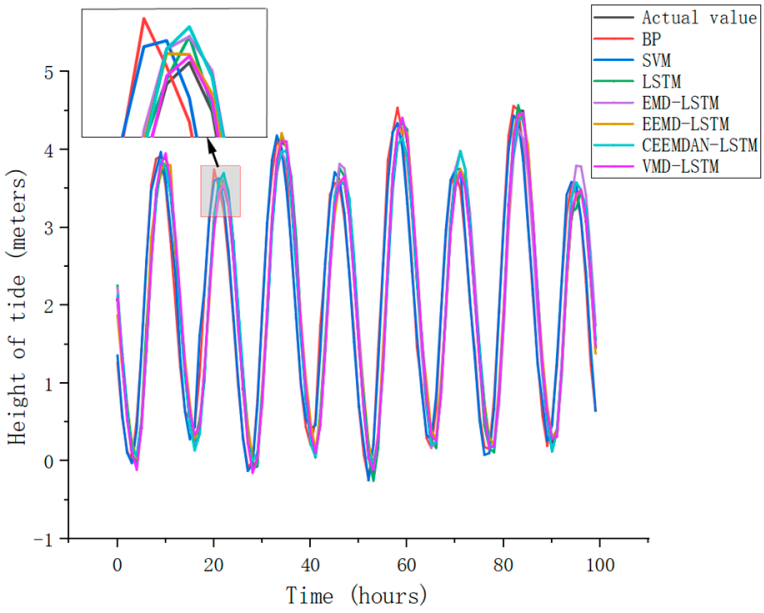

Figure 9. Comparison of VMD-LSTM with other models.

To provide a more objective and comprehensive assessment of the predictive performance of each model, four evaluation metrics were selected to evaluate the forecasting effectiveness: Root Mean Square Error (RMSE), Mean Absolute Error (MAE), Mean Absolute Percentage Error (MAPE), and Coefficient of Determination (R^2), as shown in Equations (12)–(15). Here, Xi represents the actual values, $\dot{X}$ represents the predicted values, n is the size of the time series, and $\overline{X}$ denotes the mean value. Smaller values for RMSE and MAE indicate more minor prediction errors, while a value closer to 1 for R^2 signifies higher prediction accuracy.

$$RMSE = \sqrt{\frac{1}{n}\sum_{i=1}^{n}\left(Xi - \dot{X}i\right)}, \tag{13}$$

$$MAE = \frac{1}{n}\sum_{i=1}^{n}\left|Xi - \dot{X}i\right|, \tag{14}$$

$$MAPE = \frac{100}{n}\sum_{i=1}^{n}\left|\frac{Xi - \dot{X}i}{Xi}\right|, \tag{15}$$

$$R^2 = 1 - \frac{\sum_{i=1}^{n}\left(Xi - \dot{X}i\right)^2}{\sum_{i=1}^{n}\left(Xi - \overline{X}\right)^2} \tag{16}$$

Table 2 presents the evaluation metrics for different models. The VMD-LSTM model consistently exhibits high prediction accuracy (RMSE = 0.0385 m, MAE = 0.0267 m, R^2 = 0.9991) across Luchao Port. Compared to the BP model, the VMD-LSTM model has reduced RSME, MAE, and MAPE by 79.42%, 83.24%, and 64.75%, respectively, and increased R^2 by 11.41%. Compared to the SVM model, the VMD-LSTM model shows reductions of 74.26%, 77.62%, and 59.36% in RSME, MAE, and MAPE, respectively, along with a 6.71% increase in R^2. Compared with the single LSTM model, the VMD-LSTM model exhibits decreases of 66.22%, 77.37%, and 48.88% in RSME, MAE, and MAPE, respectively, and an increase of 2.98% in R^2. In comparison to both the EMD-LSTM, EEMD-LSTM, and CEEMDAN-LSTM models, accuracy evaluation indexes exhibit significant improvements. Compared to the CEEMDAN-LSTM model, the VMD-LSTM model achieved an average reduction of 28.3% in RMSE, 37.2% in MAE, and an average improvement of 0.3% in R^2. Compared with the EMD–LSTM model, the VMD–LSTM model exhibited even more

significant improvements in the accuracy of its prediction, with a reduction of 59.2% in the RMSE, a reduction of 66.8% in the MAE, and an increase of 0.9% in the R^2.

Table 2. Evaluation indicators of different prediction models (the improvement in accuracy of the VMD-LSTM model over the EMD-LSTM model is denoted by I_1, while I_2 and I_3 represent the corresponding improvement over the EEMD-LSTM and CEEMDAN-LSTM models, respectively).

Evaluation Index	Prediction Model							Improvement Ratio		
	BP	SVM	LSTM	EMD-LSTM	EEMD-LSTM	CEEMDAN-LSTM	VMD-LSTM	I_1	I_2	I_3
RSME (m)	0.1871	0.1496	0.114	0.0943	0.0537	0.093	0.0385	59.2%	28.3%	58.6%
MAE (m)	0.1594	0.1193	0.1003	0.0805	0.0425	0.076	0.0267	66.8%	37.2%	64.9%
MAPE/%	16.551	14.354	11.412	9.136	8.585	8.862	5.8327	36.2%	32.1%	34.2%
R^2	0.8968	0.9363	0.9702	0.9905	0.9963	0.9949	0.9991	−0.9%	−0.3%	−0.4%

Therefore, in this study, the approach of decomposing the original tidal series using the VMD algorithm, with each modal component used as an independent input to forecast separately, was used. Finally, the prediction results were superposed, which could effectively improve the prediction accuracy and verify the effectiveness of this model.

4. Discussion

VMD can effectively extract the characteristics of each frequency band in the tidal data and predict the characteristics of each frequency band, respectively, which solves the problem of mode aliasing existing in EMD, EEMD, and other EMD methods and can effectively improve the prediction accuracy of the model. LSTM can solve the problems of gradient explosion and gradient disappearance problems in RNN, and is very suitable for tidal time-series data with strong time dependence. This study combines the advantages of the modal decomposition algorithm and neural network model to achieve a good prediction effect. All the experimental results show that combining the VMD algorithm and LSTM model is an ideal tidal prediction method.

The VMD algorithm can decompose the signal according to the time scale characteristics of the data itself and decompose the complex and nonlinear tide time series into a finite number of inherent modal components and trend components. The features of the decomposed sequences are different, respectively, implying different parts of the original signal's features, reducing the data's complexity. Compared with the direct use of the BP, SVM, and LSTM models for prediction, using the decomposed data can make the neural network model better capture the data features in the tide time series, reduce noise interference, and significantly improve the prediction accuracy.

VMD shows good performance in processing non-stationary and nonlinear signals. The algorithm goes through a continuous cycle to find the best solution for VMD. Due to the continuous iteration of the algorithm, the mode function generated by the analysis signal and the center frequency are also constantly updated. Its core purpose is to decompose the original time-series signal into several intrinsic mode functions (IMF) with different bandwidth constraints that fluctuate around the center frequency. At the same time, VMD-LSTM completely overcomes many drawbacks of EMD-like methods, such as endpoint effect and mode component aliasing, so that VMD-LSTM can achieve higher prediction accuracy than EMD-LSTM, EEMD-LSTM, and CEEMDAN-LSTM.

Due to the limited access to data, we only conducted a prediction study on this one place. In subsequent studies, we will collect more tidal level data from observation points for further tests to verify the generalization ability of this model.

5. Conclusions

This study focused on the tidal data from Luchao Port to address the instability and complexity issues in tidal time-series prediction. The paper proposes a predictive

model that combines variational mode decomposition (VMD) and long short-term memory (LSTM), resulting in the following conclusions:

1. Utilizing the VMD method, the tidal level data of Luchao Port is decomposed into four modal components (*IMF*), which reduces the complexity of the original tidal level data and makes the data series stable. LSTM neural network model is used to predict the IMF_i obtained from VMD, respectively, and then these prediction results are superposed, effectively improving the prediction accuracy.
2. After VMD, the prediction error of the LSTM model is reduced. Compared with the six prediction modes, the BP, SVM, LSTM, EMD-LSTM, VMD-LSTM, EEMD-LSTM, and CEEMDAN-LSTM models, the VMD-LSTM model has the smallest error, and the highest predictive accuracy, with a RMSE of 0.0385 m, MAE of 0.0267 mm, and R^2 of 0.9991.

The research proposed that the VMD-LSTM tidal prediction model provides an effective approach to forecasting, offering valuable insights for understanding tidal variations.

Author Contributions: Conceptualization, S.H.; methodology, H.N.; software, H.C.; validation, H.N.; formal analysis, H.C.; data curation, Z.X.; writing—original draft preparation, J.J.; writing—review and editing, S.H. and H.C.; funding acquisition, H.N. and H.C. All authors have read and agreed to the published version of the manuscript.

Funding: This work was funded by Zhejiang Provincial Natural Science Foundation under Grant LZJWY22E090007 and ZCLQ24E0901.

Data Availability Statement: The data that support the findings of this study are available from Shanghai Pudong New Area Hydrology and Water Resources Management Affairs Center. Restrictions apply to the availability of these data, which were used under licence for this study. Data are available from the authors with the permission of Shanghai Pudong New Area Hydrology and Water Resources Management Affairs Center.

Acknowledgments: The authors would like to thank Shanghai Pudong New Area Hydrology and Water Resources Management Affairs Center for providing us with the datasets.

Conflicts of Interest: The authors declare no conflicts of interest.

References

1. Li, L.B.; Wu, W.H.; Zhang, W.J.; Yin, J.C.; Zhu, Z.Y. Real-time Tide Level Prediction Model Based on Improved Nonlinear Auto Regressive Models Neural Network with Exogenous Inputs. *Sci. Technol. Eng.* **2022**, *22*, 9728–9735. [CrossRef]
2. Meena, B.; Agrawal, J. Tidal Level Forecasting Using ANN. *Procedia Eng.* **2015**, *116*, 607–614. [CrossRef]
3. Pan, M.; Zhou, H.; Cao, J.; Liu, Y.; Hao, J.; Li, S.; Chen, C.-H. Water Level Prediction Model Based on GRU and CNN. *IEEE Access* **2020**, *8*, 60090–60100. [CrossRef]
4. Liu, C.; Yin, J.C. A high-accuracy short-term tide prediction model. *J. Shanghai Marit. Univ.* **2016**, *37*, 74–80. [CrossRef]
5. Luo, J.M.; Jiang, Y.P.; Pang, L.; Feng, J.D. Numerical simulation of storm surge in the coast of Zhejiang based on parametric wind field model. *Haiyang Xuebao* **2022**, *44*, 20–34. [CrossRef]
6. Yin, C.; Huang, H.; Wang, D.; Liu, Y.; Guo, Z. The Characteristics of Storm Wave Behavior and Its Effect on Cage Culture Using the ADCIRC plus SWAN Model in Houshui Bay, China. *J. Ocean Univ. China (Ocean. Coast. Sea Res.)* **2020**, *19*, 307–319. [CrossRef]
7. Yang, H.; Wu, Q.; Li, G. A multi-stage forecasting system for daily ocean tidal energy based on secondary decomposition, optimized gate recurrent unit and error correction. *J. Clean. Prod.* **2024**, *449*, 141303. [CrossRef]
8. Zhang, Z.; Zhang, L.; Yue, S.; Wu, J.; Guo, F. Correction of nonstationary tidal prediction using deep-learning neural network models in tidal estuaries and rivers. *J. Hydrol.* **2023**, *622*, 129686. [CrossRef]
9. Liu, Q.; Sun, X.Q. Harmonic analysis and forecast of tides in Qingdao Port. *J. Mar. Meteorol.* **2022**, *42*, 99–106. [CrossRef]
10. Cai, S.; Liu, L.; Wang, G. Short-term tidal level prediction using normal time-frequency transform. *Ocean Eng.* **2018**, *156*, 489–499. [CrossRef]
11. Monahan, T.; Tang, T.; Adcock, T.A. A hybrid model for online short-term tidal energy forecasting. *Appl. Ocean Res.* **2023**, *137*, 103596. [CrossRef]
12. Wang, C.H. A model of the Harmonic analysis of tides. *Mar. Forecast.* **1995**, *4*, 71–76. [CrossRef]
13. Yin, J.-C.; Wang, N.-N.; Hu, J.-Q. A hybrid real-time tidal prediction mechanism based on harmonic method and variable structure neural network. *Eng. Appl. Artif. Intell.* **2015**, *41*, 223–231. [CrossRef]
14. Pan, Z.; Liu, H. Impact of human projects on storm surge in the Yangtze Estuary. *Ocean Eng.* **2020**, *196*, 106792. [CrossRef]
15. Zhang, Z.G.; Yin, J.C.; Liu, C.H. Modular Real-Time level Prediction Based on Grey-GMDH. *Period. Ocean. Univ. China* **2018**, *48*, 140–146. [CrossRef]

16. Kavousi-Fard, A. A Hybrid Accurate Model for Tidal Current Prediction. *IEEE Trans. Geosci. Remote Sens.* **2016**, *55*, 112–118. [CrossRef]
17. Li, M.C.; Liang, S.X.; Sun, Z.C.; Zhang, G.Y. Tidal Level and Current Prediction on the Basis of Data-Driven Model. *Trans. Beijing Inst. Technol.* **2010**, *30*, 864–868. [CrossRef]
18. Yan, Z.; Lu, X.; Wu, L. Exploring the Effect of Meteorological Factors on Predicting Hourly Water Levels Based on CEEMDAN and LSTM. *Water* **2023**, *15*, 3190. [CrossRef]
19. Mandal, S.; Shanas, P.; Yuvaraj, S.; Joseph, D.; Aravind, P.; George, J.; Singh, J.; Kumar, V.S. Evaluating the estuarine tidal discharge through water stage component analysis and in-situ measurement—Case study Mandovi–Zuari estuary of Goa, India. *Reg. Stud. Mar. Sci.* **2023**, *66*, 103124. [CrossRef]
20. He, F.; Wang, R.R.; Wang, J.Z. A kind of short-term height-prediction of tidal level of rivers based on BP neural network model. *J. Yangze River Sci. Res. Inst.* **2011**, *28*, 21–24. [CrossRef]
21. Yao, S.Y.; Li, G.F.; Qian, R.Z.; Wang, Y.D.; Ma, F. Tidal level forecast of Yangtze River at the source of East Route of South-to-North Water Transfer Project. *South-North Water Transf. Water Sci. Technol.* **2021**, *19*, 1136–1146. [CrossRef]
22. Di Nunno, F.; de Marinis, G.; Gargano, R.; Granata, F. Tide Prediction in the Venice Lagoon Using Nonlinear Autoregressive Exogenous (NARX) Neural Network. *Water* **2021**, *13*, 1173. [CrossRef]
23. Li, C.; Gao, F.; Wang, H.Q. Improved Fruit Fly Optimization Algorithm for Optimizing Time Series Prediction Model of CIAO-LSTM Network. *Comput. Eng. Appl.* **2020**, *56*, 129–134. [CrossRef]
24. Ye, S.; Jiang, J.G.; Li, J.J.; Liu, Y.L.; Zhou, Z.Z.; Liu, C. Fault diagnosis and tolerance control of five-level nested NPP converter using wavelet packet and LSTM. *IEEE Trans. Power Electron.* **2019**, *35*, 1907–1921. [CrossRef]
25. Wu, J.; Hu, K.; Cheng, Y.; Zhu, H.; Shao, X.; Wang, Y. Data-driven remaining useful life prediction via multiple sensor signals and deep long short-term memory neural network. *ISA Trans.* **2019**, *97*, 241–250. [CrossRef]
26. Yang, X.K.; Tang, G.; Li, D.G. Tidal level prediction and analysis based on LSTM neural network. *Port Sci. Technol.* **2022**, *5*, 39–46. [CrossRef]
27. Liu, Y.Y.; Zhang, L.; Li, L.; Liu, Y.S.; Chen, B.W.; Zhang, H.W. Storm surge nowcasting based on multivariable LSTM neural network model. *Mar. Sci. Bull.* **2020**, *39*, 689–694.
28. Xu, X.W.; Chen, Y.P.; Gan, M.; Liu, C.; Zhou, H.J. Hybrid model for short-term prediction of tide level in estuary based on LSTM and non-stationary harmonic analysis. *Mar. Sci. Bull.* **2022**, *41*, 401–410. [CrossRef]
29. Giaremis, S.; Nader, N.; Dawson, C.; Kaiser, C.; Nikidis, E.; Kaiser, H. Storm surge modeling in the AI era: Using LSTM-based machine learning for enhancing forecasting accuracy. *Coast. Eng.* **2024**, *191*, 104532. [CrossRef]
30. Ian, V.-K.; Tang, S.-K.; Pau, G. Assessing the Risk of Extreme Storm Surges from Tropical Cyclones under Climate Change Using Bidirectional Attention-Based LSTM for Improved Prediction. *Atmosphere* **2023**, *14*, 1749. [CrossRef]
31. Liu, J.; Shi, G.Y.; Zhu, K.G.; Zhang, J.W.; Li, S.H.; Chen, Z.H.; Wang, W. A combined tide prediction model based on harmonic analysis and ARIMA-SCR. *J. Shanghai Marit. Univ.* **2019**, *40*, 93–99. [CrossRef]
32. Huang, N.E.; Shen, Z.; Long, S.R.; Wu, M.C.; Shih, H.H.; Zheng, Q.; Yen, N.-C.; Tung, C.C.; Liu, H.H. The empirical mode decomposition and the Hilbert spectrum for nonlinear and non-stationary time series analysis. *Proc. R. Soc. Lond. Ser. A Math. Phys. Eng. Sci.* **1998**, *454*, 903–995. [CrossRef]
33. Wu, L.L.; Yin, L.L.; Ren, Q.L. A Short-Term Traffic Flow Forecasting Method Based on EMD and DE-BPNN Combined Optimization. *J. Chongqing Univ. Technol. (Nat. Sci.)* **2021**, *35*, 155–163. [CrossRef]
34. Ren, Z.; Hou, J.; Wang, P.; Wang, Y. Tsunami resonance and standing waves in Hangzhou Bay. *Phys. Fluids* **2021**, *33*, 081702. [CrossRef]
35. Wang, R.M.; Xie, N.; Yu, H.Y.; Yu, J.; Jiang, L.; Yang, H.Y. Short-term Load Forecasting Method Based on EMD-LSTM Model. *Res. Explor. Lab.* **2022**, *41*, 62–66. [CrossRef]
36. Yin, J.; Wang, H.; Wang, N.; Wang, X. An adaptive real-time modular tidal level prediction mechanism based on EMD and Lipschitz quotients method. *Ocean Eng.* **2023**, *289*, 116297. [CrossRef]
37. Lv, T.; Tao, A.; Zhang, Z.; Qin, S.; Wang, G. Significant wave height prediction based on the local-EMD-WaveNet model. *Ocean Eng.* **2023**, *287*, 115900. [CrossRef]
38. Wang, Z.; Wang, Q.; Wu, T. A novel hybrid model for water quality prediction based on VMD and IGOA optimized for LSTM. *Front. Environ. Sci. Eng.* **2023**, *17*, 88. [CrossRef]
39. Zhang, J.; Xin, X.; Shang, Y.; Wang, Y.; Zhang, L. Nonstationary significant wave height forecasting with a hybrid VMD-CNN model. *Ocean Eng.* **2023**, *285*, 115338. [CrossRef]
40. Wang, J.; Bethel, B.J.; Xie, W.; Dong, C. A hybrid model for significant wave height prediction based on an improved empirical wavelet transform decomposition and long-short term memory network. *Ocean Model.* **2024**, *189*, 102367. [CrossRef]
41. Ban, W.; Shen, L.; Lu, F.; Liu, X.; Pan, Y. Research on Long-Term Tidal-Height-Prediction-Based Decomposition Algorithms and Machine Learning Models. *Remote Sens.* **2023**, *15*, 3045. [CrossRef]
42. Chen, H.; Huang, S.; Xu, Y.; Teegavarapu, R.S.V.; Guo, Y.; Nie, H.; Xie, H. Using Baseflow Ensembles for Hydrologic Hysteresis Characterization in Humid Basins of Southeastern China. *Water Resour. Res.* **2024**, *60*, e2023WR036195. [CrossRef]
43. Meng, Z.; Wang, Y.; Zheng, S.; Wang, X.; Liu, D.; Zhang, J.; Shao, Y. Abnormal Monitoring Data Detection Based on Matrix Manipulation and the Cuckoo Search Algorithm. *Mathematics* **2024**, *12*, 1345. [CrossRef]
44. Yang, H.Y.; Zhao, X.Y.; Wang, L. Review of Data Normalization Methods. *Comput. Eng. Appl.* **2023**, *59*, 13–22. [CrossRef]

45. Li, Q.; Luo, Y.; Zhang, M.L. LoRaWAN water quality adaptive monitoring system based on LSTM energy prediction. *Internet Things Technol.* **2023**, *13*, 8–12. [CrossRef]
46. Zhao, J.; Xie, Z.X.; Liu, S.X. Tide prediction accuracy improvement method research based on VMD optimal decomposition of energy and GRU recurrent neural network. *Chin. J. Sci. Instrum.* **2023**, *44*, 79–87. [CrossRef]
47. Jiange, J.; Liqin, Z.; Senjun, H.; Qianqian, M. Water quality prediction based on IGRA-ISSA-LSTM model. *Water Air Soil Pollut.* **2023**, *234*, 172. [CrossRef]